Clinical Proteomics Journal

ISSN 1542-6416/04/01:69–80/$25.00

Molecular Targets

Differential Phosphoprofiles of EGF and EGFR Kinase Inhibitor-Treated Human Tumor Cells and Mouse Xenografts

David R. Stover,[*1,3] Jennifer Caldwell,[1] Jarrod Marto,[1] Karen Root,[1] Juergan Mestan,[2] Michael Stumm,[2] Olga Ornatsky,[1] Chris Orsi,[1] Nina Radosevic,[1] Linda Liao,[4] Doriano Fabbro,[2] and Michael F. Moran[4]*

[1]MDS Proteomics Inc., 1670 Discovery Dr., Charlottesville, VA and 251 Attwell Drive, Toronto M9Q 7H4, Canada
[2]Oncology Research, Novartis Pharma AG, CH-4002, Basel, Switzerland
[3]Oncology Research, Novartis Institutes for Biomedical Research, Cambridge, MA 02139
[4]Banting and Best Department of Medical Research, University of Toronto, 112 College St., Toronto, ON, M5G 1L6, Canada

Abstract

The purpose of this phospho-proteomics study was to demonstrate the broad analysis of cellular protein phosphorylation in cells and tissue as a means to monitor changes in cellular states. As a cancer model, human tumor-derived A431 cells known to express the epidermal growth factor receptor (EGFR) were grown as cell cultures or xenograft tumors in mice. The cells and tumor-bearing animals were subjected to treatments including the EGFR-directed protein kinase inhibitor PK166 and/or EGF stimulation. Whole cell/tissue protein extracts were converted to peptides by using trypsin, and phosphorylated peptides were purified by an affinity capture method. Peptides and phosphorylation sites were characterized and quantified by using a combination of tandem mass spectroscopy (MS) and Fourier transform MS instrumentation (FTMS). By analyzing roughly 10^6 cell equivalents, 780 unique phosphopeptides from approx 450 different proteins were characterized. Only a small number of these phosphorylation sites have been described previously in literature. Although a targeted analysis of the EGFR pathway was not a specific aim of this study, 22 proteins known to be associated with EGFR signaling were identified. Fifty phosphopeptides were found changed in abundance as a function of growth factor or drug treatment including novel sites of phosphorylation on the EGFR itself. These findings demonstrate the feasibility of using phospho-proteomics to determine drug and disease mechanisms, and as a measure of drug target modulation in tissue.

*Author to whom all correspondence and reprint requests should be addressed:
E-mail: David.Stover@Pharma.Novartis.Com

Key Words: Phosphoproteomics; proteomics; Fourier transform mass spectrometry (FTMS); Epidermal Growth Factor Receptor (EGFR); PKI166.

Introduction

The wide range of cellular processes that are known to involve protein phosphorylation as central elements of their regulation suggest that a clearer picture of these events would be valuable in understanding cellular physiology. Recent reports have highlighted several techniques demonstrating, to various degrees, an ability to broadly catalog many protein phosphorylation sites *(1–3)*. We have employed a modified immobilized metal affinity chromatography (IMAC) approach first reported by Ficarro et al. *(1)* in a series of differential analyses to identify phosphorylation events that occur following treatment of A431 cells with epidermal growth factor (EGF) or the EGF receptor (EGFR)-directed protein kinase inhibitor, PKI166. By analyzing sample aliquots representing roughly 10^6 cell equivalents, 780 unique phosphopeptides from approx 450 different proteins were characterized. In these phosphoproteins, all three phospho-amino acids were observed in their expected physiological ratios—the great majority being phosphoserines. Only a small number of these phosphorylation sites have been described previously in the literature. Whereas a targeted analysis of the EGFR pathway was not a specific aim of this study, 22 proteins from the EGFR pathway were identified as being phosphorylated, including six sites of phosphorylation on the EGFR itself. Three novel sites of phosphorylation were identified on the EGFR, two of which were differentially phosphorylated in response to EGF and PKI166 treatment. Using a custom-built Fourier transform mass spectrometer (FTMS), approx 350 phosphopeptides were quantified in terms of their relative abundance as a function of growth factor and drug treatment. Fifty of these peptides were found to be differentially phosphorylated by a significant amount, including differential phosphorylation on the EGFR as noted above. Overall, the results that we report provide a representative subset of the phosphoproteome that responds to PKI166 treatment and is involved in EGFR signaling and further validates the utility of this approach for identifying phosphorylation sites and their involvement in both physiological and pathophysiological processes.

The general schema for differential phosphoprofiling is depicted in Fig. 1. Protein is extracted from cell or tissue lysates and digested with trypsin. Acidic residues are derivatized to form d0 or d3 labeled methyl esters. For protein identification the individual samples are subjected to IMAC to isolate phosphopeptides and analyzed with a 4 h liquid chromatography (LC) gradient on a Q-Star Pulsar using a data dependent tandem mass spectrometry (MS/MS) algorithm. The data are then searched against public databases using Mascot to identify peptide sequences, sites of phosphorylation, and tentative protein IDs. These data are then manually checked for added veracity.

For determining relative abundance between two samples, differentially labeled samples are pooled prior to IMAC isolation of phosphopeptides and subsequent analysis is performed on a custom-built 7T FTMS. Differentially labeled pairs are identified based on their mass difference of a multiple of three and relative abundance is expressed as a ratio. Phosphopeptide identities are then assigned to specific differential ratios based on alignment of the elution times of abundant marker proteins.

The EGF pathway was chosen to demonstrate the utility of this approach to pharmaceutical research. Overexpression of the EGFR was described to be associated with nonsmall cell lung carcinomas and brain, bladder,

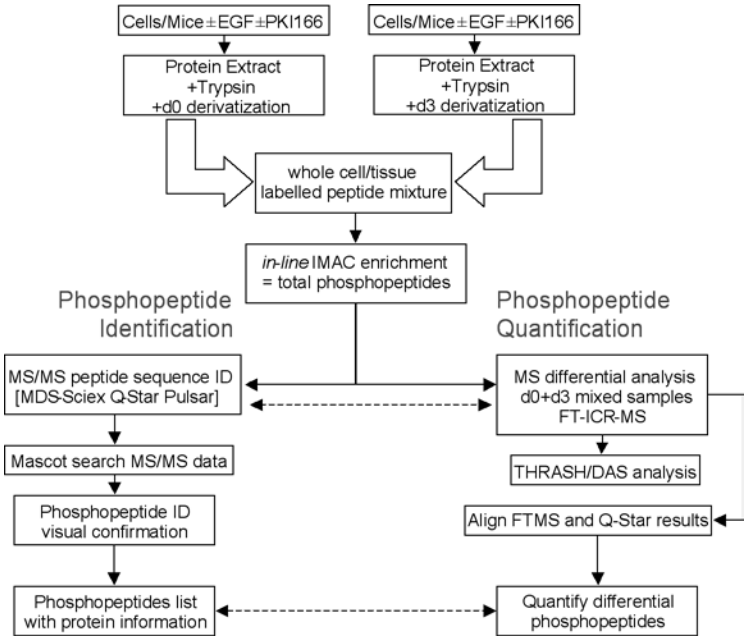

Fig. 1. Schematic of workflow for cell/animal protocols, sample preparation, and peptide and data analysis. Dashed lines show where data from one process was matched to the other to allow identification of quantified phosphopeptides.

breast, and ovarian carcinomas *(4–8)*. Deregulation (constitutive activation) of EGFR is also associated with tumorigenesis and progression *(9)*. ErbB2, most closely related to EGF-R, is overexpressed in approx 25% of primary breast and ovarian tumors; ErbB2 overexpression in these two tumor types correlates with earlier relapse and poor prognosis *(10,11)*. A number of therapeutic strategies aimed at blocking EGFR activity have been pursued, the most advanced of which include extracellularly directed antibodies that block ligand binding, Cetuximab (Erbitux) and ABX-EGF, and small molecule ATP-competitive antagonists, Iressa *(12)*, and Tarceva *(13)*.

PKI166 is a substituted pyrrolo[2,3-*d*]pyrimidine and is another ATP-competitive EGFR inhibitor, which exhibits dual inhibition of EGFR and erbB-2 (IC_{50} = 1 and 11 n*M*, respectively) *(14–16)*. PKI-166 has shown significant and dose-dependent in vivo anti-tumor activity in several EGFR expressing xenograft models in nude mice following oral administration of 10–100 mg/kg/d*(17)*. Complete and long-lasting inhibition of EGF-stimulated EGFR autophosphorylation in tumors was observed following administration of a single 100 mg/kg oral dose *(18)*. This study examines the effect of EGF and PKI166 on the phosphoprofile of the epidermoid tumor-derived A431 cell line in culture and in xenograft tumors grown in nude mice.

Results

Four samples were prepared from both cultured cells and dissected tumors, treated and analyzed as indicated in Table 1.

Table 1
Treatment, Labeling, and Differential Analysis Performed for Each Sample*

Sample	EGF	PKI	Label	p-peptides sequenced	p-sites identified	Proteins identified	pS's	pT's	pY's
T1	-	-	d3	230	330	136	188	8	2
T2	+	-	d0	98	157	59	79	7	
T3	+	1h	d3	163	207	53	141	6	
T4	+	24h	d0	76	123	55	55	2	
C1	-	-	d0	87	172	67	74	7	
C2	+	-	d3	135	**345**	85	**126**	**10**	**2**
C3	+	300 nM	d0	218	345	135	200	13	
C4	+	3000nM	d0	85	130	47	74	6	1

*Samples T(1-4) are from tumors and C(1-4) are from cultured cells (*see* Experimental Protocol for details).

The results from the phosphopeptide identification analyses are summarized in Table 1. It is important to note that these statistics are based solely on those peptides that were selected (by the MS software) for sequencing and found to have a confirmed sequence from the Mascot search. Roughly equal numbers of phosphorylation sites were identified from in vivo samples as were found the cell culture samples.

The ratio of the different phosphoamino acids (pS to pT to pY) is very similar between all samples and is consistent with expected physiological ratios. In total, 780 unique phosphopeptides were sequenced and identified from 441 different proteins. Quantitation ratios for 354 unique phosphopeptides from 117 different proteins were generated by matching differentially labeled pairs from the FTMS analysis to corresponding MS/MS data from the Q-Star analysis.

Routinely, greater than 95% of the peptides identified after the modified IMAC enrichment procedure are determined to be phosphorylated. Many more differentially labeled pairs are observed in the FTMS analysis than can be matched to Q-Star identifications, suggesting that these numbers still represent just a small percentage of the phosphopeptides.

A diverse array of proteins were determined to be phosphorylated, including: signaling molecules, kinase, phosphatases, transcription factors, proteins involved in differentiation and apoptosis, RNA processing proteins, and metabolic enzymes (Table 2). Each protein on this list was identified by MS/MS sequencing of at least one phosphopeptide with a sequence that matches a tryptic peptide within the protein. In many cases multiple phosphorylation sites were identified for each protein. For example, six sites of phosphorylation were identified within the EGFR itself, including three novel phosphoserine sites.

Whereas the actual identification of any specific phosphoprotein is a statistical event dependent upon selection by the MS software algorithm for sequencing, the numbers of proteins identified per class should be roughly proportional to their diversity, abundance, and phosphorylation status. Thus, the representation of phosphoproteins uniquely identified in the cell line samples compared to the tumor samples (Table 2) highlights the greater representation of desmosomal and gap junction phosphoproteins in the tumor cells. This observed difference can be postulated to reflect the morphology of a solid tumor com-

Table 2
Proteins Identified to be Phosphorylated in A431 Cell Cultures (In Vitro) or in A431 Tumors Grown as Xenografts in Nude Mice (In Vivo)

	Kinases P'ases	Signaling molecules	Trans. factors/ polymerases	Differentiation /apoptosis	Protein synthesis	Desmosome and cell junction	RNA proc. proteins	vesicle trafficking/ proteosome	Cytoskel.	Metab.
In vitro	CDC2L5	**ADAM17**	HECH	EIF4	ABCF1		HNRPA1	AAK1	ADD2	ACAC
	CRK7	AKAP13	FAIM	APACD	SKIV2L		NSSR	TLOC1	ADD3	ACAS2
	TJP2	**ARHGEF6**	**JunB**	BTF			PR264		BFSP1	ASR2B
	PTPN12	ARHGEF7	MLL/GMPS	EBP1			REPS1		DNCH1	Ferritin
		CARD10	PPIG	PDCD4			SFRS1		EML4	MMPL1
		CD2AP	PSIP1				SFRS10		EPB41L1	XRN2
		CNK1	SAF-B				SFRS7		PPFIA1	
		ESG3	TIAF1				SMN2		SPTBN1	
		LISCH7					SR-A1			
		OSTF1					ZNF265			
		PRKCBP1								
		RANBP3								
		SDC3								
		ZYX								
In vivo	**ABL1**	14-3-3	CENPA	Dlk1	BOP1	DSC1	DDX16	p47	COL12A1	ACLY
	BCKDK	CABIN1	D53	Dscr1l1	EIF3S8	DSC2	HNRPD	SEC61B	DBN1	ENSA
	MARK2	**G3BP**	GTF3C1	MECP2	IF2	envoplakin	SF2	SNX2	LASP1	PCYT1A
	PAK2	GNL1	H1FX	NCOR2		**JUP**	SF3B1		MAP4	PCYT1B
	PDK1	HEF1	HOXA5	NDRG1		LAD1	SKIV2L		**MLCB**	PHE1A
	PRKAA1	IL8RB	LISCH7	SNIP1		NCL	SMN		MYO9A	SGPP1
		Leucokinin	NFATC4			PKP1			TTN	
		OSBPL11	PARD3							
		PDAP1	POLR2A							
		PTGFRN	SMARCC1							
		SFN	SMARCC2							
		SPAG9	SON							
		TA4	TAB182							
			TCEB3							
			TRIM29							
Both	**EGFR**	ARPP-16	MATR3	ACINUS	DNAJC5	**AHNAK**	DKC1	CANX	COL17A1	PDHA1
		ARPP-19	PDCL2	PDCD5	EEF1D	DSG1	HNRPDL	GOLGA4	CTNNA1	PPP1R7
		CARHSP1	CBX3		**EIF4G1**	**DSP**	HNRPK	TPD52L1	**CTNND1**	TPI1
		CTNNB1	HDGF		HSP27	epiplakin1	hnrpup2		**EMS1**	
		DEK	HTX		HSP90B	LMNA	HSU53209		EPLIN	
		MARCKS	JUNB		HSPB1	PKP3	NSSR		ITGB4	
		MLP	LMNA		HSPCB	PLEC1	RBM14		SCEL	
		PDAP1	MCM2		RPLP0		RBM15			
		Sam68	PML		RPLP1		RNPC2			
		STMN1	PTRF		RPLP2		SFRS6			
		TNKS1BP1	RBBP6		**RPS6**		SFRS9			
		TRAP150	SNW1		SSB		SRRM1			
		USP8	TMPO		TEBP		SRRM2			

pared to a monolayer of cultured cells, and provides an example to support the notion that broad phosphoprotein analysis offers the potential of an unbiased view of the physiological status of a cell or tissue.

Because we compared cell states ±EGF or ±PKI166, we cataloged the phosphoproteins identified that have a known connection to the EGFR signaling pathway (Table 2). Approximately 22 proteins that are known to be associated with EGFR signaling were determined to be phosphorylated in at least one sample (shown in bold). This includes EGFR itself and several downstream kinases such as Abl, Pak2, PDK1, and RSK. Eight of these proteins were determined to be differentially phosphorylated in response to EGF and/or PKI166 treatment.

Table 3
Differentially Phosphorylated Peptides in In Vitro A431 Samples

PI	Name (Gene/protein)	Peptide sequence with Phosphosites: (* = multiple possible positions)	Positions of PhosphoSites	RATIO +/-EGF	+EGF RATIO -/+PKI 0.3mM	+EGF RATIO -/+PKI 3.0mM
563192	RPS6	RLpSpSLRApSTSK	S(235) S(236) S(240)		429.24	
679951	KRT5	TSFTSVpSR	S(36)		22.05	
116881	SRRM2	NHpSGpSRpTPPVALNSSR	S(2100) S(2102) T(2104)		7.69	
585605	PDCL2	RDpSDpSEGD	S(234) S(236)		7.07	
785555	Unknown (protein	pSESAPTLHPYSPLpSPK	S(100) S(113)		5.20	
67842	EGFR	MHLPpSPTDpSNFYR	S(967) S(971)	8.00	4.00	
67843	EGFR	MHLPpSPTDpSNFpYR	S(967) S(971) Y(974)	>3		
752666	CRK7	ESKGpSPVFLPR	S(477)		3.84	
437680	MGC2641	KRpSEGFSMDR	S(352)		3.82	
599232	TPI1	KQpSLGELIGTLNAAK	S(21)		3.18	
679951	KRT5	ISISTSGGpSFR	S(82)		0.36	
750968	na	pSAPApSPTHPGLMSPR	S(299) S(303)		0.33	
679951	KRT5	QSpSVSFR	S(6)		0.30	
104490	PPFIA1	RSpSDGpSLSHEEDLAK	S(239) S(242)		0.30	
116881	SRRM2	pSRpSPpSSPELNNK	S(1497) S(1499) S(1501)		0.21	
106162	TRAP150	RIDIpSPSTFR	S(682)		0.19	
102687	Rps6	LSpSLRApSTSK	S(236) S(240)		0.07	
120264	HSU53209	RpSPpSPYYSR	S(260) S(262)			4.80
102688	RPS6	RLpSpSLRApSTSK	S(235) S(236) S(240)			0.35
119342	DRIM	ELGILpSKIpSKFMK	S(1337) S(1340)			0.30
563192	RPS6	RLpSpSLRApSTSK	S(235) S(236) S(240)	9.97		
97007	AHNAK	HRpSNpSFSDER	S(1167) S(1169)	4.84		
457783	TFPT	LLPYPTLApSPApSD	S(240) S(243)	3.82		
103309	ADAM17	pSEKAASFK	S(803)	3.38		
104634	CDC2L5	pSRpSPYpSPVLR	S(395) S(397) S(400)	3.34		
355819	EMS1	AKpTQTPPVpSPAPQPTEER	T(362) S(368)	3.00	2.08	

Peptides that were determined to be significantly differentially phosphorylated in at least one of the cell line comparisons are listed in Table 3. A number of phosphopeptides are observed to be more abundant in EGF treated (+) vs untreated (–) A431 cells. Specifically, an EGFR peptide containing two novel phosphoserines is eightfold more abundant in EGF treated cells, while 300 n*M* PKI166 (cell 2) inhibited formation of this phosphopeptide by a factor of 4, suggesting that regulation of S967 and S971 phosphorylation is stimulated by EGF and inhibited by PKI166. Because PKI166 is a relatively selective EGFR inhibitor, the observed inhibition of phosphorylation of these sites is probably a result of inhibition of EGFR pathways leading to activation of serine kinases and/or serine phosphatases, rather than direct effects on those enzymes.

This same peptide was found to be phosphorylated on tyrosine, corresponding to EGFR Y974, after treatment with EGF. No signal was detected for this phosphopeptide in the absence of EGF treatment; therefore, the

differential ratio is recorded as greater than the difference between the signal observed in '+' (d3 label) and the background level.

The largest finite difference measured was that of ribosomal protein S6. With almost a 10-fold increase in EGF treated vs nontreated and over a 400-fold increase in cells treated with EGF alone compared to those treated with EGF and 300 n*M* PKI166 (Table 3), phosphorylation of this peptide is clearly affected by the status of EGFR signaling and modulation by PKI166. The three phosphorylation sites identified on this peptide correspond to phosphorylation sites on ribosomal protein S6 known to correlate with activation of protein synthesis *(19,20)*.

To highlight one complication of quantifying phosphopeptides, it should be pointed out that a related phosphopeptide from RPS6 was determined to be >10-fold more abundant in PKI166 treated cells than in cells treated with EGF alone (differential ratio of 0.07). Because this peptide contains two of the same phosphoserines as the peptide described above (pS236 and pS240), this data would appear to be contradictory. However, upon careful inspection this data is consistent with the expected pattern of EGF stimulation of RPS6 phosphorylation and inhibition of RPS6 phosphorylation by PKI166. Briefly, the RPS6 phosphopeptide carrying two phosphosites is decreased because of increased phosphorylation of a third serine (pS235). This third phosphorylation also results in a change in the trypsin cleavage site.

ADAM 17 (A disintegrin and metalloproteinase domain 17) also known as TNF-α converting enzyme (TACE) has multiple splice variants. One splice variant lacks residues 656...827, we found S786 to be phosphorylated, thereby identifying the presence of the long splice variant. TACE regulates EGFR ligand availability in vivo *(21)*. We found phosphorylation of S786 to be inhibited in the presence of EGF. This suggests the possibility of a novel mechanism regulating TACE mediated production of EGFR ligands through a feedback mechanism.

Cdc2-related kinase 7 (Crk7) also called CDC2 related kinase with an arginine/serine-rich (RS) domain (CrkRS), is a 1490 amino acid protein that contains RS domains similar to that of RNA splicing factors and co-localizes with a hyperphosphorylated form of RNA Polymerase II in cells and phosphorylates RNA Polymerase II in vitro *(22)*. Thus Crk7 may be a link between transcription and splicing machinery. In this study, phosphorylation of Crk 7 on S477, was inhibited by a factor of 3.84 by 300 n*M* PKI166 treatment. S477 is located within a PEST-like sequence suggesting a possible role for this phosphorylation in regulating Crk7 degradation in response to EGF.

CDC2-Like kinase 5 (CDC2L5) or CDC2 Related Kinase 5 (Crk5) is the full-length amino acid sequence of the cholinesterase-related cell division controller (CHED) kinase, a previously published partial coding sequence23. This ubiquitous nuclear protein, shares a PITAVRE and PITAIRE motif with other Cdc2-related proteins. Antisense-CHED treatment impairs growth and/or differentiation of hematopoietic cells (megakaryocytes), indicating that CHED is a positive growth/differentiation regulator *(24)*. The kinase domain of CDC2L5 is 89% identical to Crk7 and it also contains a Ser-Arg-rich (RS) domain that may play a role in nuclear localization of the protein. Serines 395, 397, and 400 are localized in the middle of the RS-rich sequence in CDC2L5. Increased phosphorylation of these serines, upon stimulation with EGF, may affect the nuclear targeting necessary for execution of CDC2L5's role in mitotic regulation.

Protein tyrosine phosphatase receptor type f polypeptide (PTPRF) or interacting protein

Table 4
Differentially Phosphorylated Peptides Identified From A431 Tumor Samples

PI	Name (Gene/protein)	Peptide sequence with Phosphosites: (* = multiple possible positions)	Positions of Phosphorylations	Ratio +/-EGF	+EGF Ratio -/+PKI 1h	+EGF Ratio +PKI 1h/24 h
78	KRT1	pSLVNLGGpSK	S(66) S(73)	3.57		
81517	DSP	AEpSGPDLR	S(22)	3.25		
100502	LASP1	RDpSQDGSSYR	S(146)	0.28		
306257	RPS6	LSpSLRApSTSK	S(236) S(240)		8.56	
1639	KRT5	FVSTTS*S*S*R	S*(582) S*(583) S*(584)		8.41	
78184	KRT6E	YTTTS*S*S*S*RKpSYKH	S*(555) S*(556) S*(557) S*(558) S(561)		4.37	
98256	CTNND1	GpSLApSLDpSLRK	S(292) S(295) S(298)		1.45	3.70
98256	CTNND1	GSLApSLDpSLRK	S(295) S(298)		0.98	4.27
78	KRT1	SGGGFSSGpSAGIINYQR	S(21)		0.69	42.59
81517	DSP	SMpSFQGIR	S(2209)		0.53	13.36
70248	SFRS1	pSPpSYGRpSR	S(199) S(201) S(205)		0.13	
48107	DSP	GLPSPYNMS*S*APGpSR	S*(1701) S*(1702) S(1706)			12.00
670031	Plakophilin 1	SSQSSTLSHpSNR	S(65)			8.52
1484	KRT6C	YTTTSSpSSR	S(557)			7.89
1484	KRT6C	YTTTSSSpSRK	S(558)			7.20
679951	KRT5	FVSTTSSpSRK	S(584)			7.10
791008	EMS1	LPpSSPVYEDAASFK	S(380)			6.41
679951	KRT5	TSFTSVpSR	S(36)			5.72
1484	KRT6C	pSLYGLGGSK	S(60)			4.93
101877	PKP1	FS*S*YS*QMENWSR	S*(118) S*(119) S*(121)			4.90
679951	KRT5	GLGVGFGSGGGSSSpSVK	S(574)			4.69
78	KRT1	pSLVNLGGSK	S(66)			4.47
679951	KRT5	ISIpSTSGGSFR	S(77)			4.22
566434	KRT6A	RGFSAS*S*AR	S*(21) S*(22)			4.05
582968	PKP3	LS*S*GFDDIDLPSAVK	S*(313) S*(314)			3.90
154127	keratin 4	pSLYNLR	S(51)			3.85
101877	PKP1	NMLGTLAGANpSLR	S(717)			3.58
582968	PKP3	LS*S*GFDDIDLPSAVK	S*(313) S*(314)			3.54
670031	Plakophilin 1	FSSYpSQMENWSR	S(121)			3.53

(liprin), α-1(PPFIA1), is a member of a receptor PTPase interacting family that binds to type f receptors such as leukocyte common antigen-related protein (LAR). PPFIA1 binds to the LAR membrane-distal D2 protein tyrosine phosphatase domain and appears to localize LAR to focal adhesions. Both LAR and PPFIA1 decorate the ends of focal adhesions most proximal to the cell nucleus and are excluded from the distal ends of focal adhesions, thus localizing to regions of focal adhesions presumably undergoing disassembly. Therefore, LAR and PPFIA1 may regulate the disassembly of focal adhesions and thus help orchestrate cell-matrix interactions. Increased phosphorylation of PPFIA1 in the presence of 300 n*M* PKI166 is consistent with the large body of literature claiming a role for EGF signaling in down regulating focal adhesions and thereby stimulating tumor invasion *(25,26)*.

The two phosphopeptides from the tumor extracts determined to be increased with EGF treatment are from Keratin (Krt1) and desmoplakin (DSP) (Table 4). Significantly, the tumor T3:T4 comparison demonstrated higher levels of phosphorylation of many desmosomal and cytoskeletal proteins (DSP, Keratins, and Plakophilins) in tumors from mice treated with

PKI166 for 1 h (T3) as compared to those treated for 24 h (T4). Similarly EMS1 (Cortactin) and catenin D1 (CTNND1) were shown to have higher levels of phosphorylation at the earlier time point. These data suggest that while EGFR itself may be maximally inhibited at 1 h (data not shown), the inhibition of downstream events affecting the cytoskeleton and gap junctions/desmosomes lags behind. Maximal inhibition of these events may require transcriptional regulation, protein turnover, and/or other processes that would follow a different time course than EGFR autophosphorylation.

Cortactin plays a role in regulating cortical actin assembly, transmembrane receptor organization and membrane dynamics. Aberrant regulation of cortactin levels contributes to tumor cell invasion and metastasis *(27)*. EGF-stimulation increases phosphorylation of cortactin two-fold on Ser/Thr residues. Mek activation is necessary and sufficient for EGF-induced phosphorylation of Cortactin *(28)*. In this study, we found increased phosphorylation of Cortactin on S368 upon EGF stimulation and reduced phosphorylation following treatment with PKI166 in vitro (Table 4). These data are consistent with disruption of the EGFR-MEK-Erk pathway leading to cortical actin rearrangements by PKI166. In vivo phosphorylation of S380 was elevated in 1 h PKI166-treated mice compared to 24 h post-PKI166 delivery. The time course of phosphoregulation of this protein mirrors that of the cytoskeletal and desmosomal proteins identified consistent with its involvement in regulating actin assembly and membrane dynamics.

P120 Catenin delta 1 (p120ctn) is implicated both in cell transformation by Src and in ligand-induced receptor signaling through the EGF, PDGF, CSF-1 and Erbb2 receptors *(29)*. The association of catenins to cadherins produces a complex which is linked to the actin filament network, and which seems to be of primary importance for cadherins cell-adhesion properties *(30)*. Consistent with a role in EGF-induced signaling, three phosphoserines in p120ctn were found to be differentially regulated in the T3:T4 comparison.

This study has further highlighted the utility of the IMAC phosphoprofiling method to catalog large numbers of cellular phosphorylation events. Furthermore, with the addition of the d0/d3 methyl ester labeling step, this method can be used to analyze relative abundance of phosphorylations in different cell states. Significantly, this report is the first to demonstrate the utility of this approach to assess in vivo phosphorylation events.

Overall, this approach offers a novel means to analyze protein function and/or drug interactions in an unbiased way. By taking a global snapshot of a large number of phosphorylation events, effects of protein function or drugs can be observed without guessing which pathways you expect might be altered. Once data from such a global analysis has been achieved then more targeted approaches, such as co-immunoprecipitations, can be done to obtain more detailed information within affected pathways.

Experimental Protocol

In Vitro A431 Samples

1×10^7 A431 cells (confluent monolayer in 75 mm dishes: approx 2×10^6 cells per 75 mm dish) were starved for 16 h in medium containing 1% fetal bovine serum (FBS), treated for 60 min with EGF (50 ng/mL) in the presence or absence of PKI166 (300 n*M*, 3000 n*M*). Cells were preincubated for 30 min with PKI166 prior to treatment with EGF.

In Vivo A431 Tumor Xenografts

The A431 epidermoid cell line (obtained from the American Type Culture Collection [CRL 1555]) was used to establish sc tumors in female BALB/c nu/nu (nude) mice according to a previously described method *(18)* and tumors

were grown to between 400 and 600 mg in mass. Based upon previous pharmacokinetic determinations PKI166-treated mice received 100 mg/kg po whereas control mice received vehicle (four mice per group). Mice were then sacrificed at 0 h, 1 h, and 24 h after cessation of treatment. Five minutes before sacrifice, the mice were administered 0.5 μg EGF/g body weight iv; a group of vehicle-treated control mice received 0.2 mL 0.9% w/v NaCl instead of EGF. The tumors were dissected free of necrotic material and then divided into halves, snap-frozen in liquid nitrogen and stored at –80°C.

Lysis and Protein Extraction

Cells or tumors were lysed and total protein extracted by using 1 mL of TRIzol Reagent (Invitrogen) per 10^7 cells or 5:1 vol:wt in the case of tumors. RNA and DNA were removed by ethanol precipitation and protein was collected by isopropanol precipitation. Protein pellets were washed with 0.3*M* guanidine-HCl in ethanol prior to protein solubilization and analysis. Tryptic digests of protein samples were derivatized in the presence of either d0 or d3 methanol as a means to differentially mass-label peptides, as indicated in Table 1. By this approach, labeled peptide mixtures were combined prior to mass spec analysis, and identical peptides differing by 3 daltons (per esterified methyl group) were identified and quantified for relative abundance.

Sample Preparation

Sample preparation followed the procedure of Ficarro et al. *(1)*. Briefly, the Trizol protein pellets were solubulized in 1% sodium dodecyl sulfate (SDS) and diluted to 0.2% SDS in digest buffer for digestion overnight with trypsin. The digests were taken to dryness and methyl esters were made using d0 or d3 methanol, as listed in Tables 1 and 2. After esterification the samples were aliquoted and taken to dryness. Aliquoted samples were stored at –80°C for future use.

IMAC Enrichment

IMAC enrichment followed the procedure of Ficarro et al. *(1)*. Each sample was subjected to IMAC phosphopeptide enrichment. A metal chelating microcapillary column was washed with ethylene diamine tetraaccetic acid (EDTA) and then charged with iron. The column was acidified and the digested sample was loaded to allow the phosphopeptides to remain on the column. Organic washes were used to remove non-phosphorylated peptides and the phosphopeptides were eluted onto a C-18 precolumn with a phosphate wash.

Qualitative MS analysis

The precolumn was attached to a C-18 analytical column with an emitter tip. The whole column is connected to an Agilent 1100 HPLC such that peptides were eluted in to the Sciex Qstar Pulsar mass spectrometer. For a qualitative look at the phosphopeptides present in a sample we used a 4 h HPLC gradient where solvent A was 0.2*M* acetic acid (HOAc) and solvent B was 0.2*M* HOAc in 70% acetonitrile (MeCN). The mass spectrometer is set to acquire MS/MS spectra on the top three most abundant ions in a MS scan. Once a mass is subjected to MS/MS it is placed on an exclusion list for 1 min to allow lesser abundant ions to be selected for MS/MS analysis.

Qualitative Data Analysis

All MS/MS spectra were searched against human-nr database using the Mascot search algorithm. The correct methyl ester, d0 or d3, was used as a static modification and differential modifications of phosphorylated Ser, Thr, and Tyr were used as search parameters. All MS/MS identifications were visually inspected and those deemed correct were added to a phosphopeptide list for each sample.

Quantitative MS Analysis

For quantitative analysis another IMAC enrichment was performed, except that two samples were mixed, one d0 and one d3 labeled sample, and then loaded onto the IMAC column for phospho enrichment. All of the peptides were eluted onto a precolumn and eluted into the mass spectrometer. Either the FTMS or the QStar Pulsar was used for this experiment. A custom-built 7T FTMS was used for this study. During gradient elution of the peptides the ions are accumulated in an external quadrupole and then are pulsed into the trap. Ions are detected for approx 100 ms/s scan event. The current FTMS only produces MS information during the 1 h HPLC gradient. The QStar Pulsar was set to acquire one MS and one MS/MS spectra during a 4 h gradient. All quantitative data is analyzed manually and with software developed at MDS Proteomics.

Acknowledgments

The authors thank Daniel Figeys and Forest White for invaluable technical contributions, and Don Hunt and Jeff Shabanowitz at the University of Virginia for their cooperation and advice related to this study.

References

1 Ficarro SB, McCleland ML, Stukenberg PT, et al. Phosphoproteome analysis by mass spectrometry and its application to *Saccharomyces cerevisae*. Nat Biotechnol 2002;19: 01-305.
2 Oda Y, Nagasu T, Chait BT. Enrichment analysis of phosphorylated proteins as a tool for probing the phosphoproteome. Nat Biotechnol 2001;19:379-382.
3 Zhou H, Watts JD,Aebersold R. A systematic approach to the analysis of protein phosphorylation. Nat Biotechnol 2001;19:375-378.
4 Yarden Y. The EGFR family and its ligands in human cancer. signalling mechanisms and therapeutic opportunities. Eur J Cancer 2001; 37:S3-S8.
5 Mendelsohn J, Baselga J. The EGF receptor family as targets for cancer therapy Oncogene 2000;19,6550-6565.
6 Voldborg B R, Damstrup L, Spang-Thomsen, M. & Poulsen, H. S. Epidermal growth factor receptor (EGFR) and EGFR mutations, function and possible role in clinical trials. Ann Oncol 1997;12:1197-1206.
7 Moscatello DK, Holgado-Madruga M, Godwin, AK, et al. Frequent expression of a mutant epidermal growth factor receptor in multiple human tumors. Cancer Res 1995;55:5536-5539.
8 Salomon DS, Brandt R, Ciardiello F, Normanno N. Epidermal growth factor-related peptides and their receptors in human malignancies. Crit Rev Oncol Hematol 1995;19:183-232.
9 Scambia G, Benedetti-Panici P, Ferrandina G, et al. Epidermal growth factor, oestrogen and progesterone receptor expression in primary ovarian cancer: correlation with clinical outcome and response to chemotherapy. Br J Cancer 1995;72:361-366.
10 Simpson BJ, Phillips HA., Lessels AM, Langdon SP, Miller WR. c-erbB growth-factor-receptor proteins in ovarian tumours. Int J Cancer 1995;64:202-206.
11 Slamon, D. J. et al. Studies of the HER-2/neu proto-oncogene in human breast and ovarian cancer. Science 1987;235:177-182.
12. Herbst RS. ZD1839: targeting the epidermal growth factor receptor in cancer therapy. Expert Opin. Invest Drugs 2002;11:837-849.
13 Moyer JD, Barbacci EG, Iwata KK, et al. Induction of apoptosis and cell cycle arrest by CP-358,774, an inhibitor of epidermal growth factor receptor tyrosine kinase. Cancer Res 1997;57:4838-4848.
14 Traxler P, Bold G, Buchdunger E, et al. Tyrosine kinase inhibitors: from rational design to clinical trials. Med Res Rev 2001;21,499-512.
15. Caravatti G, Bruggen J, Buchdunger E, et al. Pyrrolo[2,3-d]Pyrimidine and Pyrazolo[3,4-d] Pyrimidine Derivatives as Selective Inhibitors of the EGF Receptor Tyrosine Kinase. ACS Symposium Series, ed. 796: Anticancer Agents. Oxford University Press, USA: 2001;231–244.
16 Bruns CJ, Solorzano CC, Harbison MT, et al. Blockade of the epidermal growth factor receptor signaling by a novel tyrosine kinase inhibitor leads to apoptosis of endothelial cells and therapy of human pancreatic carcinoma. Cancer Res 2000;60,2926-2935.

17 Brandt R, Wong AML, Hynes NE. Mammary glands reconstituted with Neu/ErbB2 transformed HC11 cells provide a novel orthotopic tumor model for testing anti-cancer agents. Oncogene 2001;20:5459-5465.
18. Baker CH, Solorzano CC, Fidler IJ. Blockade of vascular endothelial growth factor receptor and epidermal growth factor receptor signaling for therapy of metastatic human pancreatic cancer. Cancer Res 2002;62:1996-2003.
19 Ferrari S, Bandi HR, Hofsteenge J, Bussian BM, Thomas G. Mitogen-activated 70K S6 kinase. Identification of in vitro 40 S ribosomal S6 phosphorylation sites. J Biol Chem 1991;266(33):22770-22775.
20 Ferrari S, Pearson RB, Siegmann M, Kozma SC, Thomas G. The immunosuppressant rapamycin induces inactivation of p70s6k through dephosphorylation of a novel set of sites. J Biol Chem 1993;268(6):4530-4533.
21. Sunnarborg SW, Hinkle CL, Stevenson M, et al. Tumor necrosis factor-α converting enzyme (TACE) regulates epidermal growth factor receptor ligand availability. J Biol Chem 2002; 277(15):12838-12845 (2002).
22. Ko TK, Kelly E, Pines J. CrkRS: a novel conserved Cdc2-related protein kinase that colocalises with SC35 speckles. J Cell Sci 2001; 114:2591-2603 (2001).
23. Marques F, Moreau JL, Peaucellier G, et al. A new subfamily of high molecular mass CDC2-related kinases with PITAI/VRE motifs. Biochem Biophys Res Commun 2000;279(3): 832-837 (2000).
24 Lapidot-Lifson Y, Patinkin D, Prody CA, et al. Cloning and antisense oligodeoxynucleotide inhibition of a human homolog of cdc2 required in hematopoiesis. Proc Natl Acad Sci USA 1992;89(2):579-583.
25 Hauck CR, Sieg DJ, Hsia DA, Loftus JC, Gaarde WA, Monia BP, Schlaepfer DD. Inhibition of focal adhesion kinase expression or activity disrupts epidermal growth factor-stimulated signaling promoting the migration of invasive human carcinoma cells. Cancer Res 2001; 61(19):7079-7090.
26 Lu L, Han AP, Chen JJ. Translation initiation control by heme-regulated eukaryotic initiation factor 2alpha kinase in erythroid cells under cytoplasmic stresses. Mol Cell Biol 2001; 12:4016-4031.
27 Weed SA, Parsons JD. Cortactin: coupling membrane dynamics to cortical actin assembly. Oncogene 2001;20:6418-6434.
28 Campbell DH, Sutherland RL, Daly RJ. Signaling pathways and structural domains required for phosphorylation of EMS1/ cortactin. Cancer Res 1999;59:5376-5385.
29 Mariner DJ. Identification of Src phosphorylation sites in the catenin p120ctn. J Biol Chem 2001;276:28006-28013 .
30. Lu Q. δ-catenin, an adhesive junction-associated protein which promotes cell scattering. J Cell Biol 1999;144:519-532.